



Pontificia Universidad Católica de Chile.
School of Engineering
Directorate for Research and Innovation
iPre Undergraduate Research Program

Modeling and Control of Magnetic Forces between Microrobots

Amelia Fernández Seguel ^a, Alejandro I. Maass^b

^a *Robotic Engineering, School of Engineering, Pontificia Universidad Católica de Chile. 2nd Year, afernan-
dezs3@estudiante.uc.cl*

^b *Department of Electrical Engineering, School of Engineering, Pontificia Universidad Católica de Chile.,
Assistant Professor, alejandro.maass@uc.cl*

Abstract

The independent control of multiple magnetic microrobots under a shared global signal presents critical challenges in biomedical applications such as targeted drug delivery and microsurgeries. Most existing systems only allow all agents to move synchronously, limiting their use in applications that require differentiated actuation.

This research aims to design a controller capable of regulating the radial distance between micro-agents using only the angle ψ of a global magnetic field as the actuation parameter, demonstrating great potential for practical applications.

The proposed cascade control approach enables faster and more precise adjustment of the inter-agent distance than a proportional controller, while maintaining smooth transitions and avoiding abrupt changes in the orientation of the **MAGNETIC FIELD**, making it suitable for real-world implementation.

To this end, a bibliographic review was first conducted to develop the physical model, considering magnetic dipole–dipole interactions and velocities in **VISCOUS MEDIA**. Subsequently, a PID controller was designed and implemented to regulate the radial distance, followed by a PD controller in cascade to smooth changes in the field’s orientation.

These controllers were simulated in MATLAB, showing that the PID controller reduced the convergence time to the desired radius by approximately 40%. When adding the second controller, the combined PID+PD scheme achieved smooth angular trajectories within similar timeframes, with fluctuations of only $\pm 5^\circ$.

These results validate the feasibility of controlling the radial distance of two microrobots using a shared magnetic field in a fast and precise manner, without abrupt variations in the control angle - an improvement over previously proposed controllers. However, the current model is limited to a 2D environment and two agents, suggesting future research to extend the controller to 3D systems and multiple agents.

Keywords: *microrobots, magnetic control, multi-agent systems, PID control, biomedicine.*

1 Introduction

Robotics has transformed numerous scientific fields, and medicine is no exception. From the introduction of automated devices in surgeries to the development of technologies for rehabilitation, the integration of robotics into medical environments has enhanced diagnosis, treatment, and overall healthcare effectiveness by enabling greater precision, reduced invasiveness, and improved clinical outcomes. (Agrawal et al., 2024)

One of the most recent examples is “Pill Bot,” an ingestible capsule robot that explores the gastrointestinal tract in real time, simplifying diagnostic procedures (Endiatx, 2025). However, future medical needs demand even smaller and more autonomous systems, which is why the concept of medical robotics is gaining increasing relevance (Dupont, 2021).

Within this context, medical robotics can be classified into three scales (Bogue, 2010):

- **Macrorobotics:** Robotic arms and prosthetic devices
- **Microrobotics:** Structures smaller than 1 mm, with cross-disciplinary applications such as minimally invasive interventions
- **Nanorobotics:** Systems for drug delivery or direct manipulation of molecular structures

Unlike macroscopic robots, microrobots are governed by microscale forces (surface tension, chemical interactions) and lack conventional actuators or sensors. Their control relies on external stimuli such as light, ultrasound, or magnetic fields (Lamkin-Kennard and Popovic, 2018). Among these, magnetic control stands out for its safety, ability to generate precise 3D forces, and compatibility with biological tissues. (Shao et al., 2021)

However, the challenge lies in independently controlling multiple magnetic microrobots under a shared global signal. Most current systems can only move all agents synchronously, which limits their application in contexts requiring individual movement. (Salehizadeh, 2020)

This research note addresses the problem of differentiated control in magnetic multi-agent systems, proposing strategies to modulate inter-agent forces and achieve selective actuation.

The ultimate goal is to develop a control system applicable to practical scenarios such as targeted drug delivery or microsurgeries, where precision and autonomy among agents are essential.

2 Initial Research

2.1 System Characteristics

The microrobots are modeled as disks with a radius of $R = 250 \mu\text{m}$ and a **MAGNETIC MOMENT** \mathbf{m} . They operate in honey to limit their degrees of freedom and minimize capillary effects, simplifying the physical model.

2.2 Forces

2.2.1 Magnetic field of a dipole

A dipolar agent (**MAGNETIC DIPOLE**) generates a magnetic field around itself, which is expressed as follows (Griffiths, 2013a):

$$\mathbf{B}_{dip}(\mathbf{r}) = \frac{\mu_0}{4\pi} \frac{1}{r^3} [3(\mathbf{m}_1 \cdot \hat{\mathbf{r}})\hat{\mathbf{r}} - \mathbf{m}] \quad (1)$$

Where:

- $\mathbf{B}_{dip}(\mathbf{r})$ is the magnetic field generated by the agent.
- \mathbf{r} is the vector from the source dipole (e.g., agent 1) to the point where the field is evaluated (e.g., agent 2).
- μ_0 is the permeability of free space ($4\pi \cdot 10^{-7} \text{H/m}$).
- r is the distance between agents.
- $\hat{\mathbf{r}}$ is a unit vector indicating the direction of \mathbf{r} .
- \mathbf{m} is the magnetic moment of the agent.

2.2.2 Permeability of the medium

The interaction between magnetic dipoles occurs through the magnetic field in the surrounding medium, which depends on the medium's magnetic permeability. This value is given by (Griffiths, 2013b):

$$\mu = \mu_0 \mu_r \quad (2)$$

Since the agents are submerged in honey, which, being organic, has a **MAGNETIC PERMEABILITY** close to 1 ($\mu_r \approx 1$), the total permeability is:

$$\mu = \mu_0 \cdot 1 = \mu_0 \quad (3)$$

Thus, the expression in (1) remains valid.

2.2.3 Forces between microrobots

Based on these parameters, the force experienced by agent 2 due to the field \mathbf{B}_{dip} (1) can be calculated as (Griffiths, 2013c):

$$\mathbf{F} = \nabla(\mathbf{m}_2 \cdot \mathbf{B}_{dip}) \quad (4)$$

To simplify control, and following assumptions made in previous studies (Salehizadeh, 2020), all magnetic moments of the microrobots are considered aligned with the applied field, denoted as \mathbf{b}_a .

Given that the agents are identical (and thus have the same magnetic moment), we define:

$$\mathbf{m}_1 = \mathbf{m}_2 = m\hat{\mathbf{b}}_a \quad (5)$$

Where \mathbf{m}_1 and \mathbf{m}_2 correspond to the moments of agents 1 and 2, and $m\hat{\mathbf{b}}_a$ represents the magnitude of the moment in the direction of \mathbf{b}_a .

Substituting these expressions into (1) and then into (4) yields:

$$\mathbf{F} = \frac{3\mu_0 m^2}{4\pi r^4} \left[(\hat{\mathbf{b}}_a \cdot \hat{\mathbf{r}})\hat{\mathbf{r}} + (\hat{\mathbf{b}}_a \cdot \hat{\mathbf{r}})\hat{\mathbf{b}}_a + (\hat{\mathbf{b}}_a \cdot \hat{\mathbf{b}}_a)\hat{\mathbf{r}} - 5(\hat{\mathbf{b}}_a \cdot \hat{\mathbf{r}})^2 \hat{\mathbf{r}} \right] \quad (6)$$

2.2.4 Local coordinates

Since $\hat{\mathbf{b}}_a$ is a unit vector representing the direction of \mathbf{b}_a , it follows that $(\hat{\mathbf{b}}_a \cdot \hat{\mathbf{b}}_a = 1)$, allowing the equation to be simplified as:

$$\mathbf{F} = \frac{3\mu_0 m^2}{4\pi r^4} \left[2(\hat{\mathbf{b}}_a \cdot \hat{\mathbf{r}})\hat{\mathbf{b}}_a + \hat{\mathbf{r}} - 5(\hat{\mathbf{b}}_a \cdot \hat{\mathbf{r}})^2 \hat{\mathbf{r}} \right] \quad (7)$$

To decompose this force into local coordinates, an orthonormal system is defined. The agents are considered to be in a water-oil medium for simplicity (Figure 1)

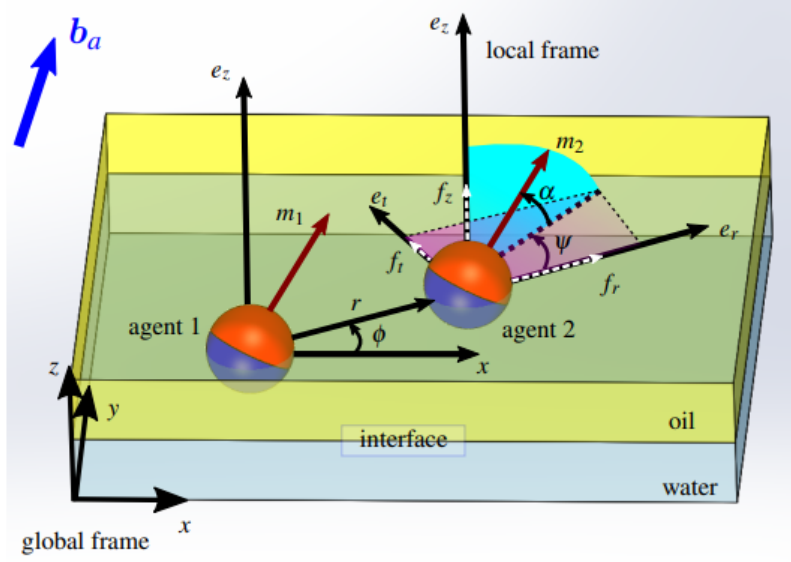


Figure 1: Representation of agent coordinates in a water–oil medium (Salehizadeh, 2020)

This system is parameterized in spherical coordinates as:

$$\hat{\mathbf{b}}_a = \cos \alpha \cos \psi \hat{\mathbf{e}}_r + \cos \alpha \sin \psi \hat{\mathbf{e}}_t + \sin \alpha \hat{\mathbf{e}}_z \quad (8)$$

Where:

- ψ : In-plane angle (xy) between the projection of \mathbf{b}_a and the radial vector $\hat{\mathbf{e}}_r$.
- α : Out-of-plane angle (z) between \mathbf{b}_a and its projection on the (xy) plane.
- $\hat{\mathbf{e}}_r = \hat{\mathbf{r}}$: Radial direction.
- $\hat{\mathbf{e}}_t$: Tangential direction in the plane, orthogonal to $\hat{\mathbf{e}}_r$.
- $\hat{\mathbf{e}}_z$: Direction perpendicular to the plane.

A spherical parameterization was used because the agents are spherical.

2.2.5 Minimum magnitude of the applied field

The magnitude of \mathbf{b}_a must ensure that the dipoles remain aligned with it, without being significantly affected by their mutual proximity. This condition is expressed as:

$$|\mathbf{b}_a|_{min} = \frac{b - \sqrt{b^2 - 4ac}}{2a} \quad (9)$$

With:

$$a = \frac{1}{(A_1)^2} - \frac{1}{(A_2)^2} \quad (10a)$$

$$b = \frac{\mu_0 \mathbf{m} \left(\frac{4}{(A_1)^2} + \frac{2}{(A_2)^2} - 3 \right)}{2\pi r^3} \quad (10b)$$

$$c = \frac{\mu_0^2 \mathbf{m}^2 \left(\frac{-4}{(A_1)^2} + \frac{1}{(A_2)^2} + 6 \right)}{16\pi r^6} \quad (10c)$$

$$A_1 = \cos(\theta_\epsilon + \cos^{-1}(A_2)) \quad (10d)$$

$$A_2 = \cos(\psi) \cos(\alpha) \quad (10e)$$

Here, θ_ϵ represents the maximum error angle. The minimum magnitude $|\mathbf{b}_a|_{\min}$ ensures that the applied field dominates local interactions, maintaining dipole alignment. The terms A_1 and A_2 capture the angular dependencies (ψ, α) and the maximum allowable error θ_ϵ .

2.2.6 Simplification under assumptions

To determine the force components along each direction, \mathbf{f}_{21} is projected onto the corresponding axes.

Radial component:

$$f_r = \mathbf{f}_{21} \cdot \hat{\mathbf{e}}_r = \frac{3\mu_0 \mathbf{m}^2}{4\pi r^4} [2(\cos \alpha \cos \psi)^2 + 1 - 5(\cos \alpha \cos \psi)^2]. \quad (11)$$

Simplified to:

$$f_r = \frac{3\mu_0 \mathbf{m}^2}{4\pi r^4} [1 - 3 \cos^2(\alpha) \cos^2(\psi)]. \quad (12)$$

Tangential component:

$$f_t = \mathbf{f}_{21} \cdot \hat{\mathbf{e}}_t = \frac{3\mu_0 \mathbf{m}^2}{4\pi r^4} [2 \cos^2 \alpha \cos \psi \sin \psi]. \quad (13)$$

Simplified to:

$$f_t = \frac{3\mu_0 \mathbf{m}^2}{4\pi r^4} \cos^2 \alpha \sin 2\psi. \quad (14)$$

Normal component:

$$f_z = \mathbf{f}_{21} \cdot \hat{\mathbf{e}}_z = \frac{3\mu_0 \mathbf{m}^2}{4\pi r^4} [2 \cos \alpha \cos \psi \sin \alpha]. \quad (15)$$

Simplified to:

$$f_z = \frac{3\mu_0 \mathbf{m}^2}{4\pi r^4} \sin 2\alpha \cos \psi. \quad (16)$$

Defining $\Omega = \frac{3\mu_0 \mathbf{m}^2}{4\pi}$, the resulting expressions can be summarized as:

$$f_r = \frac{\Omega}{r^4} [1 - 3 \cos^2 \alpha \cos^2 \psi], \quad (13.1)$$

$$f_t = \frac{\Omega}{r^4} \cos^2 \alpha \sin 2\psi, \quad (13.2)$$

$$f_z = \frac{\Omega}{r^4} \sin 2\alpha \cos \psi. \quad (13.3)$$

The resulting force depends on the relative orientation between the applied magnetic field and the position of the second agent with respect to the first.

The equations obtained are consistent with those presented in the reference thesis (Salehizadeh, 2020).

2.3 Velocities

2.3.1 Radial velocity

Given that the microrobots operate in a viscous environment at a microscopic scale, their behavior is governed by **STOKES' LAW** (King, 2002):

$$f_m = 6\pi\mu_m Rv \quad (18)$$

Where:

- μ_m is the viscosity of the medium,
- R is the radius of the agent,
- v is the displacement velocity.

Solving for velocity:

$$v = \frac{f_m}{6\pi\mu_m R} \quad (19)$$

And defining $\sigma_{tras} = 6\pi\mu_m R$ as a constant:

$$v = \frac{f_m}{\sigma_{tras}} \quad (20)$$

This equation can be substituted to obtain the radial velocity:

$$\dot{r} = \frac{f_r}{\sigma_{tras}} = \frac{\Omega}{\sigma_{tras} r^4} [1 - 3 \cos^2 \alpha \cos^2 \psi] \quad (21)$$

and defining:

$$\Omega_t = \frac{\Omega}{\sigma_{tras}} = \frac{\frac{3\mu_0 m^2}{4\pi}}{6\pi\mu_m R} = \frac{\mu_0 m^2}{8\pi^2 \mu_m R} \quad (22)$$

to obtain

$$\dot{r} = \frac{\Omega_t}{r^4} [1 - 3 \cos^2 \alpha \cos^2 \psi] \quad (23)$$

2.3.2 Angular velocity

In the case of $\dot{\phi}$, torque must be taken into consideration. The tangential force (f_t) generates a torque that makes the agent rotate around the center of mass, this is given by:

$$\tau_{drag} = f_t \cdot r \quad (24)$$

The rotational Stokes' law (Happel and Brenner, 1983) indicates that in viscous fluids (as would be the case with honey), the following holds:

$$\tau_{drag} = \sigma_{rot} \cdot \dot{\phi} \quad (25)$$

Where $\sigma_{rot} = 8\pi\mu R^3$. By equating these two equations:

$$\sigma_{rot} \cdot \dot{\phi} = f_t \cdot r \quad (26)$$

We solve for:

$$\dot{\phi} = \frac{f_t \cdot r}{\sigma_{rot}} \quad (27)$$

When replacing with (13.2):

$$\dot{\phi} = \frac{\Omega \cos^2(\alpha) \sin(2\psi)}{r^3 \cdot \sigma_{rot}} \quad (28)$$

These expressions, by defining $\Omega_t = \frac{\Omega}{\sigma_{tras}}$ and $\Omega_r = \frac{\Omega}{\sigma_{rot}}$, can be summarized as:

$$\dot{r} = \frac{\Omega_t}{r^4} [1 - 3 \cos^2 \alpha \cos^2 \psi], \quad (29a)$$

$$\dot{\phi} = \frac{\Omega_r}{r^3} [\cos^2(\alpha) \sin(2\psi)]. \quad (29b)$$

With $\Omega = \frac{3\mu_0 m^2}{4\pi}$, $\sigma_{tras} = 6\pi\mu_m R$ and $\sigma_{rot} = 8\pi\mu_m R^3$, where $\mu_0 = 4\pi \cdot 10^{-7} \frac{H}{m}$, m corresponds to the magnetic moment of the agents, R to the radius of the agents, μ_m to the viscosity of the medium.

Table 1 summarizes the key physical constants that will be used for the controller design.

Constant	Value	Unit	Description
μ_0	$4\pi \cdot 10^{-7}$	H/m	Permeability of free space
m	$6.545 \cdot 10^{-7}$	A·m ²	Magnetic moment of the microrobot
R	$250 \cdot 10^{-6}$	m	Radius of the microrobot
μ_m	0.5	Pa·s	Viscosity of the medium (honey)
σ_{tras}	$6\pi\mu_m R$	N·s/m	Translational friction constant
σ_{rot}	$8\pi\mu_m R^3$	N·m·s	Rotational friction constant
ψ_s	54.74	degrees	Angle at which RADIAL FORCE ≈ 0

Table 1: Physical parameters of the microrobot and its environment

3 Control

The following presents the design, simulation, and validation of the control to regulate the radial distance between agents. First, the problem of **UNDERACTUATION** (Section 3.1) is analyzed, where a single parameter (ψ) controls multiple variables (r, ϕ). Then, in Section 3.2, the proportional controller (P) is evaluated, to later develop and implement the improved PID controller (Section 3.3) and its cascade version with PD. Finally, Section 3.4 discusses limitations and future extensions.

3.1 Underactuated Motion

Using the information mentioned in Section 2 on velocities, a control can be created to manage the distance at which the agents are located. In this case, only the angle ψ is considered as the control signal, assuming that $\alpha = 0^\circ$.

$$\dot{r} = \frac{\Omega_t}{r^4} [1 - 3 \cos^2(\psi)] , \quad (30a)$$

$$\dot{\phi} = \frac{\Omega_r}{r^3} [\sin(2\psi)] \quad (30b)$$

Since the agents will be aligned with the field b_a , its direction can be used to control the behavior between the agents. Using the polarities, the following three cases are defined, which can be observed in Figure 2.

1. Maximum attraction ($\psi = 0^\circ$): When this occurs, the attraction is maximum, with $\dot{r} = -\frac{2\Omega_t}{r^4}$ and $f_r = -\frac{2\Omega}{r^4}$.
2. Maximum repulsion ($\psi = 90^\circ$): When this occurs, the repulsion is maximum, with $\dot{r} = \frac{\Omega_t}{r^4}$ and $f_r = \frac{\Omega}{r^4}$.
3. Zero force ($\psi = 54.74^\circ$): At this specific angle, $\dot{r} = 0.0002 \cdot \frac{\Omega_t}{r^4}$, considered as zero velocity.

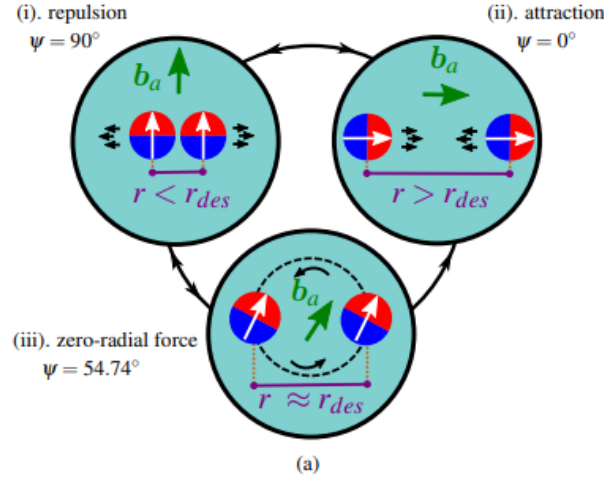


Figure 2: Principle of radial distance control of micro-agents using the angle ψ as the effector parameter (Salehizadeh, 2020)

Taking the above into account, it is possible to use this information to define a control system. Based on what is stated in (9), a value ϵ is defined, representing the minimum allowed distance radius between agents, such that the field \mathbf{b}_a is capable of aligning them with itself and the model is applicable.

r_{min} and r_{max} are also defined as limits within which the created controller has greater effectiveness. Outside these values, maximum attraction or repulsion forces are applied.

From the aforementioned, a piecewise controller can be generated:

$$\dot{r} = \begin{cases} \frac{\Omega_t}{r^4} & \epsilon < r < r_{min} \rightarrow (\psi = 90) \\ f_{\text{intermediate}}(r, \psi) & r_{min} \leq r \leq r_{max} \rightarrow (\psi = [0, 90]) \\ -\frac{2\Omega_t}{r^4} & x > r_{max} \rightarrow (\psi = 0) \end{cases} \quad (31)$$

Where $f_{\text{intermediate}}(r, \psi)$ represents the controller that is yet to be defined, with the objective of adjusting the distance precisely and smoothly within the optimal operating range.

This controller will use the angle ψ of the field \mathbf{b}_a , considering that the force is null when $\psi = 54.74^\circ$.

This specific value is obtained by solving the equation $\dot{r} = \frac{\Omega_t}{r^4}[1 - \cos^2(\psi)] = 0$, implying that $\cos^2(\psi) = \frac{1}{3}$ and therefore $\psi \approx 54.74^\circ$. At this angle, the radial force is nullified, allowing a constant distance between agents to be maintained.

The formulas given in (30) describe not only the distance r , but also the rate of change of ϕ . Since this is an underactuated system controlled only by ψ , the states r and ϕ are coupled; when adjusting ψ to correct the radius, ϕ will be affected.

One possibility to regulate ϕ without affecting r is to take advantage of the trigonometric dependence of the forces:

- r depends on $\cos^2(\psi)$, symmetric in ψ
- ϕ depends on $\sin(2\psi)$, asymmetric in ψ

With this, a Bang-Bang type control can be implemented, that is, a controller that rapidly alternates between two states, to change the sign of ψ (positive and negative) and thus obtain the desired value of ϕ . To do this, once the desired radius is obtained, the field b_a is applied with $\psi = \pm 54.74^\circ$ to only affect the angle ϕ of the agents.

3.2 Existing P Control

3.2.1 Generalities

In a doctoral thesis by Mohhammad Salehizadeh (Salehizadeh, 2020), a proportional controller is applied to regulate the angle of the field b_a in the interval $[r_{min}, r_{max}]$. For this, a radial error was defined as $\epsilon_r = r - r_{desired}$, allowing a P-type control to be directly applied:

$$\psi = \psi_s - K||\epsilon_r|| \quad (32)$$

Where ψ_s corresponds to the angle of 54.74° , at which the applied force is null. The value of the constant K was apparently configured manually.

It was considered that the given value of ψ be in the interval $[0, 90]$ when defining r_{min} and r_{max} indicated in the piecewise controller (31).

Once the corresponding radius is obtained, the value of the angle in the **APPLIED MAGNETIC FIELD** (b_a) is varied to $\psi = \pm 54.74$ until the desired value of ϕ is obtained.

To study the behaviour of this type of controller, simulations were carried out in MATLAB R2024b, replicating its operation under specific conditions.

3.2.2 Constants

First, the value of the constants used was defined. For this, the following calculations were made, considering the values of Ω , σ_{tras} and σ_{rot} defined in (29).

For Ω_t :

$$\Omega_t = \frac{\Omega}{\phi_{tras}} = \frac{\frac{3\mu_0 \mathbf{m}^2}{4\pi}}{6\pi\mu_m R} = \frac{\mu_0 \mathbf{m}^2}{8\pi^2\mu_m R} = \frac{4\pi \cdot 10^7 \frac{H}{m} \mathbf{m}^2}{8\pi^2\mu_m R} = \frac{5 \cdot 10^{-8}}{\pi} \cdot \frac{\mathbf{m}^2 \frac{H}{m}}{R \cdot \mu_m} \quad (33)$$

For Ω_r :

$$\Omega_t = \frac{\Omega}{\phi_{tras}} = \frac{\frac{3\mu_0 \mathbf{m}^2}{4\pi}}{8\pi\mu_m R^3} = \frac{3\mu_0 \mathbf{m}^2}{32\pi^2\mu_m R^3} = \frac{3 \cdot 4\pi \cdot 10^{-7} \frac{H}{m} \mathbf{m}^2}{32\pi^2\mu_m R^3} = \frac{3 \cdot 10^{-7}}{8\pi} \cdot \frac{\mathbf{m}^2 \frac{H}{m}}{R^3 \cdot \mu_m} \quad (34)$$

The values of \mathbf{m}^2 and R (magnetic moment and radius) will depend on the agent to be controlled, and μ_m will depend on the viscosity of the medium used. In the case that the same agents proposed in the thesis are used, we will have:

- $R = 250\mu m$
- $|M| = 10^4 \frac{A}{m}$
- Because the magnetic moment of a dipole is given by $\mathbf{m} = M \cdot V$ where V is the volume, the following calculation is performed: $\mathbf{m} = M \cdot \frac{4}{3}\pi R^3 = 10^4 [\frac{A}{m}] \cdot \frac{4}{3}\pi \cdot (250 \cdot 10^{-6} [m])^3 \approx 6.545 \cdot 10^{-7} [A \cdot m^2]$
- μ_m is not fixed, it corresponds to the viscosity of the medium, which is not explicitly stated in the thesis read

When substituting into the simplified equation for Ω_t :

$$\Omega_t = \frac{5 \cdot 10^{-8}}{\pi} \cdot \frac{\mathbf{m}^2 \frac{H}{m}}{R \cdot \mu_m} = \frac{5 \cdot 10^{-8}}{\pi} \cdot \frac{(6.545 \cdot 10^{-7} [A \cdot m^2])^2 [\frac{H}{m}]}{250 \cdot 10^{-6} [m] \cdot \mu_m} \approx 2,7271 \cdot 10^{-17} \cdot \frac{1}{\mu_m} [HA^2 m^2] \quad (35)$$

And for Ω_r :

$$\Omega_t = \frac{3 \cdot 10^{-7}}{8\pi} \cdot \frac{\mathbf{m}^2[\frac{H}{m}]}{R^3 \cdot \mu_m} = \frac{3 \cdot 10^{-7}}{8\pi} \cdot \frac{(6.545 \cdot 10^{-7}[A \cdot m^2])^2[\frac{H}{m}]}{(250 \cdot 10^{-6})^3 \cdot \mu_m} \approx 3.2725 \cdot 10^{-10} \cdot \frac{1}{\mu_m} [HA^2] \quad (36)$$

3.2.3 Parameters

Based on these calculations, the parameters used in the simulation were defined: the micro-robot radius was considered equal to $250 \cdot 10^{-6}$, m, the magnetic moment was $6.545 \cdot 10^{-7}$, A \cdot m², and the viscosity of the medium was set at $\mu_m = 0.5$, Pa \cdot s. Furthermore, the value of Ω_t was determined as $\Omega_t = \frac{2.7271 \cdot 10^{-7} [HA^2 m^2]}{\mu_m}$.

The controller limits and the desired radius were fixed, while the only variable parameter was the initial radius. The values considered were: $r_{min} = 300 \cdot 10^{-6}$, m, $r_{max} = 700 \cdot 10^{-6}$ m, $k_p = 0.2$ and $r_{des} = 500 \cdot 10^{-6}$ [m].

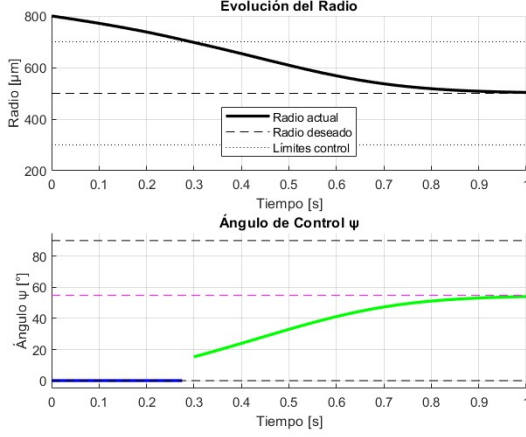
Additionally, a saturator was incorporated to restrict the angle calculated by the controller to a range between 0° and 90°, since values outside that interval contradict the system's principles (Figure 2).

3.2.4 Simulation

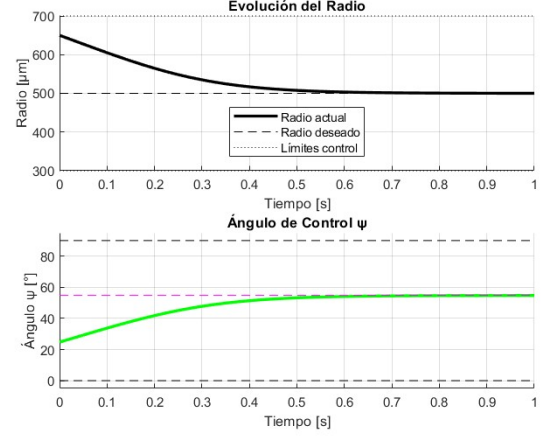
Four different cases were analysed according to the value of the initial radius r_0 :

- Outside the upper range, $r_0 = 800 \cdot 10^{-6}$ [m] (3a)
- Inside the range but greater than the desired radius, $r_0 = 650 \cdot 10^{-6}$ [m] (3b)
- Inside the range but less than the desired radius, $r_0 = 350 \cdot 10^{-6}$ [m] (3c)
- Outside the lower range, $r_0 = 200 \cdot 10^{-6}$ [m] (3d)

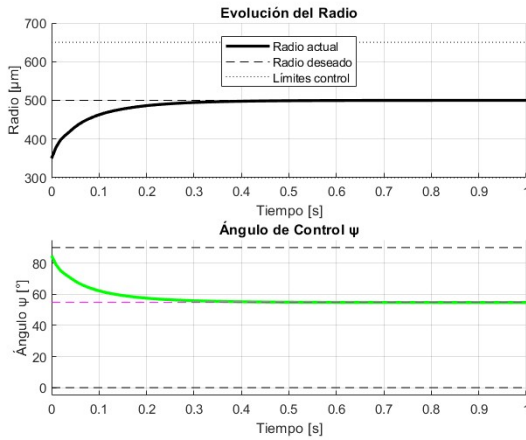
With Figure 3, it can be observed that, although the system does not present steady-state error and the radius and angle curves are smooth, without excessive oscillations, the time it takes to reach the desired value is considerably high in proportion to the distance variation.



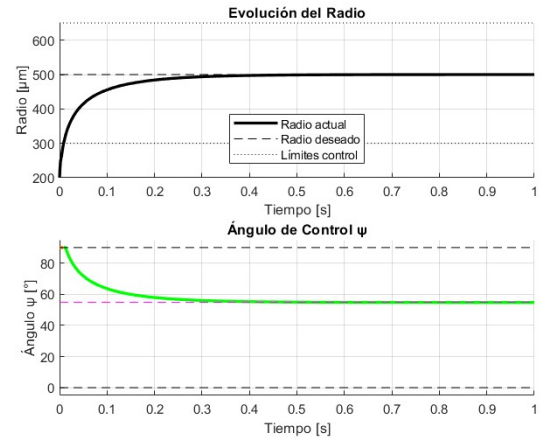
(a) r_0 outside the upper range



(b) r_0 inside the range and greater than r_{des}



(c) r_0 inside the range and less than r_{des}



(d) r_0 outside the lower range

Figure 3: Simulation of radial distance change with P-type controller

3.3 Proposed Controller

3.3.1 PID

To achieve a smoother and more efficient control response, a **PID controller** was initially proposed. The goal was to reach the desired radius more rapidly while maintaining the precision already achieved with the proportional controller.

For this purpose, the code previously used in the proportional controller simulation was adapted to include a linearized PID controller (Appendix A.2), with the following terms:

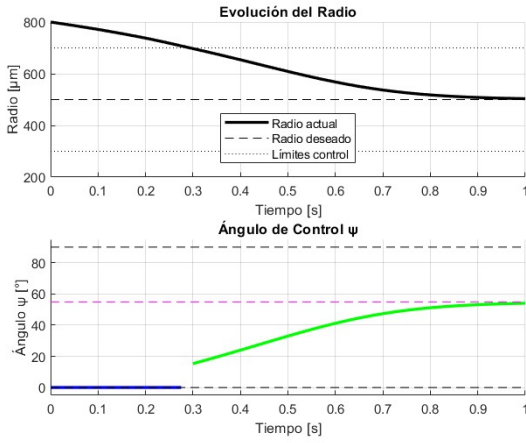
$$\psi_p = k_p \cdot error_r \psi_i = \psi_i + k_i \cdot error_r \psi_d = k_d \cdot (error_r - error_{previous}) \quad (37)$$

Considering that the base angle—where the applied force is practically null according to (30a) - corresponds to 54.74° , the total control angle was defined as:

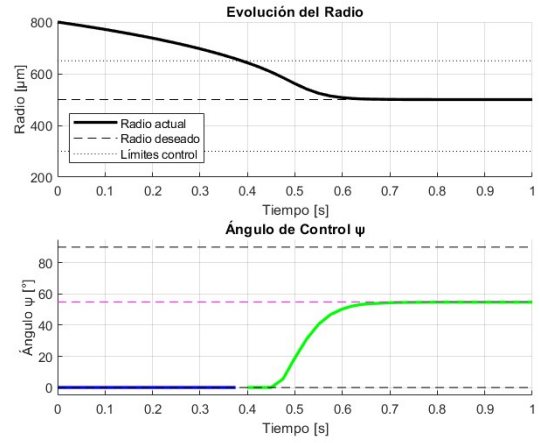
$$\psi = 54.74 - (\psi_p + \psi_i + \psi_d) \quad (38)$$

The parameters k_p , k_i , and k_d were manually tuned. The process began by maintaining the same k_p as in the proportional controller simulation, then progressively increasing the integral and derivative terms until a stable and smooth response was obtained.

The results were compared under the same conditions as those described in Figure 3, but using both the proportional and PID controllers. These comparisons are presented in Figures 4, 5, 6, and 7.

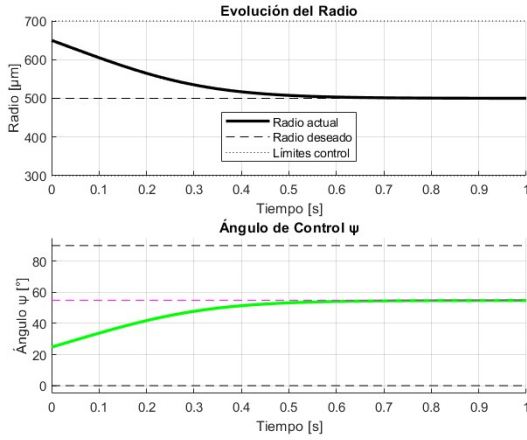


(a) Simulation with proportional control

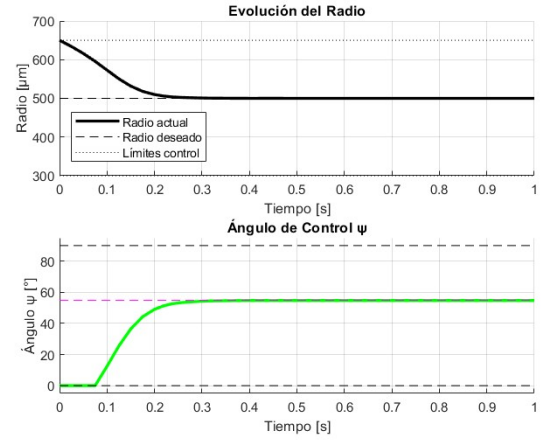


(b) Simulation with PID control

Figure 4: Comparison of controllers with r_0 outside the upper range

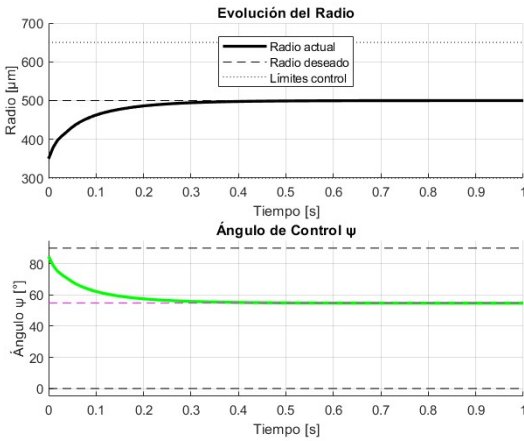


(a) Simulation with proportional control

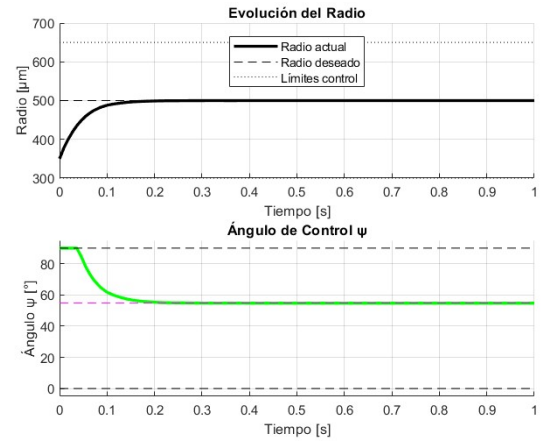


(b) Simulation with PID control

Figure 5: Comparison of controllers with r_0 inside the range and greater than desired

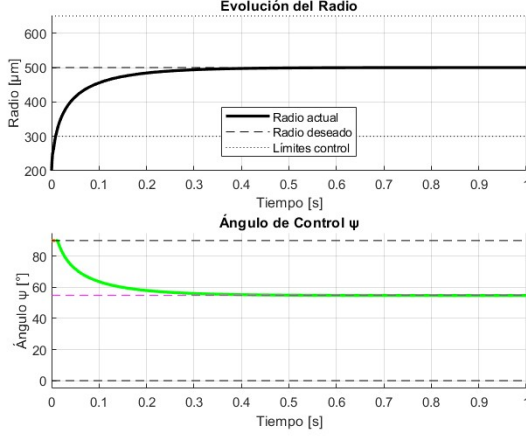


(a) Simulation with proportional control

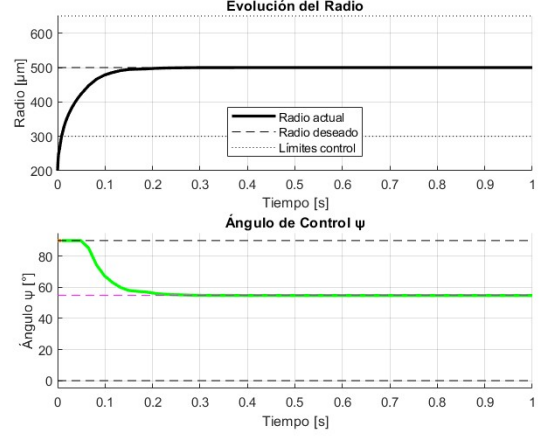


(b) Simulation with PID control

Figure 6: Comparison of controllers with r_0 inside the range and less than desired



(a) Simulation with proportional control



(b) Simulation with PID control

Figure 7: Comparison of controllers with r_0 outside the lower range

The results show that the PID controller achieves the desired radius faster without generating oscillations that significantly affect either the angle or the radius, demonstrating a clear improvement over proportional control. Furthermore, note that at the beginning of Figures 4a and 4b, the blue line in the angle plot indicates that the value computed by the controller temporarily exceeds the limits defined by r_{min} and r_{max} - a situation handled by the previously implemented saturator.

The visible jump in this same simulation arises because the plot is in discrete time; those milliseconds represent the moment when the saturator stops acting and only the controller is active.

In these tests, a single value for the initial and desired radius was used. To assess system performance under dynamic target variations, an additional simulation was conducted (Appendix A.3), where the desired radius changes every second. The initial radius was $r_0 = 800 \cdot 10^{-6}[m]$, with the following sequence of targets:

$$50 \cdot 10^{-6}[m], 400 \cdot 10^{-6}[m], 600 \cdot 10^{-6}[m], 550 \cdot 10^{-6}[m], 450 \cdot 10^{-6}[m]$$

Figures 8 and 9 show the results.

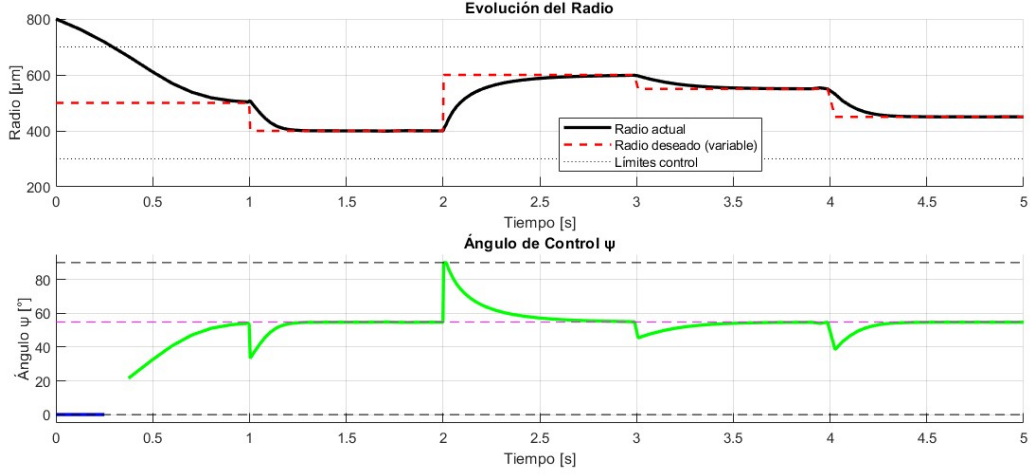


Figure 8: Simulation of proportional control applied to multiple target radii

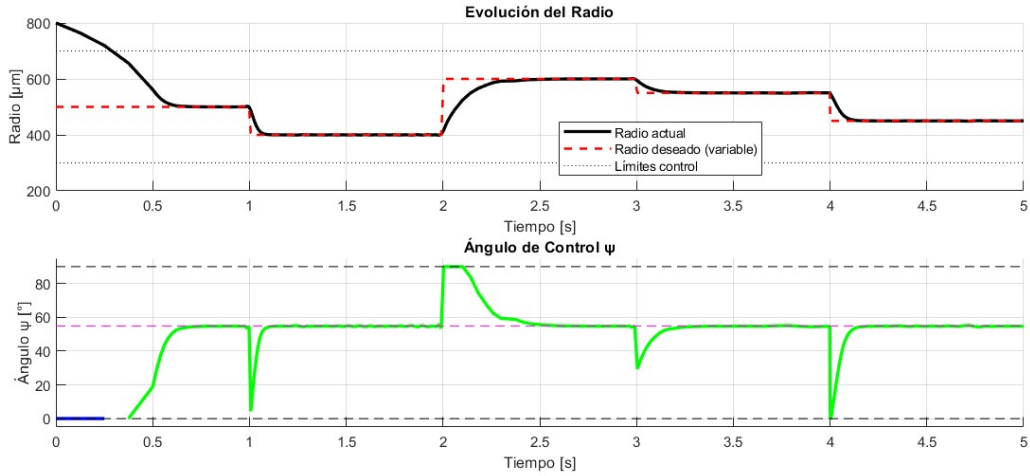


Figure 9: Simulation of PID control applied to multiple target radii

The PID controller adapts quickly to each new target, accurately reaching all of them. In contrast, during the first change, the proportional controller fails to reach the target before the next update, demonstrating the PID's advantage in dynamic conditions.

However, this improvement in precision and response speed introduces a new challenge related to the rate of change of the field angle. In particular, the PID controller produces abrupt angular variations. The simulation does not account for the actual physical time required for the microrobot to rotate, nor for mechanical constraints on such rapid reorientations.

To address this, a second controller was designed to smooth the angular evolution, ensuring a continuous and realistic trajectory.

3.3.2 Cascade

To smooth these abrupt angular changes, a PD controller was implemented (Appendix A.4), which considers both the angle computed by the previous controller and the angle applied in the previous time step. This second control layer is executed immediately after the PID, serving as an additional stage to improve signal continuity.

The integral term was omitted, as steady-state error is not a major concern here, and its inclusion could introduce unnecessary instability.

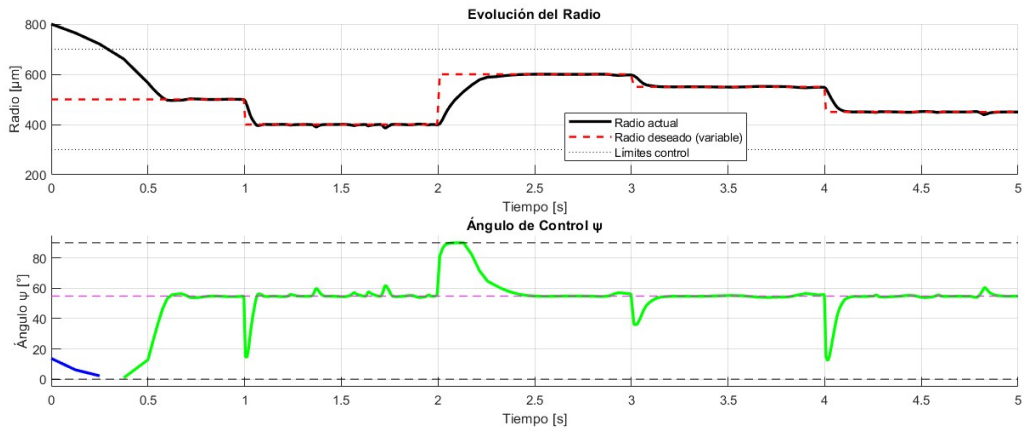


Figure 10: Simulation of the cascade controller (PID + PD) applied to multiple target radii

As shown in Figure 10, while the angle still fluctuates, these variations are substantially smoother compared to using only the PID controller.

The pronounced peaks were attenuated, reducing abrupt changes and avoiding extreme angles (0° or 90°), resulting in a more realistic and feasible control scheme for future physical applications. The additional controller did not significantly increase computation time.

Although the radius presents slight fluctuations, they remain minimal.

A classic control architecture combining PID and PD was selected mainly for its straightforward implementation, intuitive physical interpretation, and robust performance in systems with non-perfectly-linear dynamics such as this one.

Specifically, the PID controller efficiently corrects errors by balancing response speed, precision, and stability, while the cascade PD provides smoothing of the control signal without

error accumulation.

Although more advanced alternatives - such as nonlinear or optimal control strategies - exist, they require more complex modeling and precise parameter estimation, which would deviate from this study's original goal: to identify a functional, simple, and robust control strategy for an underactuated system under idealized conditions.

3.4 Future Work

While the proposed controller performs well under the analyzed conditions, its applicability is limited to 2D systems and considers only the angle ψ as a control parameter acting on two agents. As the number of agents increases, controller effectiveness decreases due to stronger coupling effects and underactuation.

Extending this controller is non-trivial, as the coupling between agents is nonlinear, and multi-agent interactions become increasingly complex, requiring a deeper analysis of the system.

Additionally, this model assumes that the normal motion component remains constant, which is valid only under the specific conditions of the medium - assumed here to be honey.

Therefore, it is proposed to study the system's sensitivity to varying viscosities, both constant and time-varying, through simulations replicating real biological fluids. This would enable evaluating controller robustness under diverse physical conditions.

Further simulations should also include external disturbances, allowing the controller to be tested for noise resistance.

Future research will focus on extending the controller to three-dimensional systems with multiple agents, including obstacle interaction and corresponding simulations. Finally, experimental validation with real agents is planned to assess performance in practical biomedical applications.

4 Conclusion

This research demonstrated the feasibility of controlling the radial distance between two agents in 2D using a shared global magnetic field, thus validating the initial hypothesis. The results showed that the PID controller reduced convergence time to the target radius by approximately 40% compared to proportional control.

Adding the cascade PD controller produced smoother angular trajectories, reducing abrupt variations to within $\pm 5^\circ$ with minimal radial deviations, making it suitable for physical implementation.

This control strategy is particularly relevant for biomedical applications requiring micrometric precision in multi-agent control, such as targeted drug delivery and minimally invasive microsurgery.

Although limited to 2D and two agents, the proposed model establishes a solid foundation for extending to 3D environments with variable viscosity and larger agent populations. It represents a well-grounded advancement in the control of underactuated microrobotic systems.

Glossary

The following glossary defines the main physical and control-related concepts used throughout this report:

1. **APPLIED MAGNETIC FIELD (\mathbf{b}_a):** External signal that orients the magnetic moments of the microrobots. It is modulated by the angles ψ and α (8).
2. **PID CONTROLLER:** Control system that combines Proportional, Integral, and Derivative actions to adjust variables such as radial distance (r).
3. **MAGNETIC DIPOLE:** Physical model representing the microrobots, characterized by their magnetic moment (m). It generates attractive or repulsive forces depending on its orientation (1).
4. **RADIAL FORCE (f_r):** Component of the force between microrobots that affects their distance. It depends on the angle ψ (12).
5. **STOKES' LAW:** Describes the motion of spheres in viscous fluids. Used to calculate radial (21) and angular velocities (25).
6. **VISCOUS MEDIUM:** Fluid (e.g., honey, $\mu_m = 0.5 [Pa \cdot s]$) where the microrobots operate, determining their dynamic friction ($\sigma_{\text{tras}}, \sigma_{\text{rot}}$ in Table 1).
7. **MAGNETIC MOMENT (m):** Vector property that quantifies the magnetic strength and orientation of a microrobot ($6.545 \cdot 10^{-7} [Am^2]$ in this research).
8. **MAGNETIC PERMEABILITY (μ):** Ability of a medium (e.g., honey) to support the formation of magnetic fields. In this research, $\mu \approx \mu_0$ (3).
9. **UNDERACTUATION:** Limitation where the number of control parameters (ψ) is smaller than the system's degrees of freedom (r, ϕ).

Acknowledgements

I would like to express my gratitude to Professor Alejandro Maass for his guidance and for opening the doors to this research, as well as to Santiago Gomez, whose initial advice was key to contacting the professor and initiating this project.

My gratitude also goes to Michel Rozas, whose enthusiasm for electrical engineering inspired me to pursue this path, and whose help in understanding certain concepts of this research offered a new perspective on our work.

I would also like to thank my father, Guillermo Fernández-Bunster, whose support in writing was invaluable in bringing clarity and coherence to each section.

Finally, I am grateful to the UC Engineering Directorate for Research and Innovation for promoting spaces such as IPre, where students can explore research beyond the visible curriculum and delve into more specialized topics.

References

- Agrawal, A., Soni, R., Gupta, D., & Dubey, G. (2024). The role of robotics in medical science: Advancements, applications, and future directions. *Journal of Autonomous Intelligence*, 7(3). <https://doi.org/10.32629/jai.v7i3.1008>
- Bogue, R. (2010). Microrobots and nanorobots: A review of recent developments. *Industrial Robot: The International Journal of Robotics Research and Application*, 37(4), 341–346. <https://doi.org/10.1108/01439911011044796>
- Dupont, P. E. (2021). A decade retrospective of medical robotics research from 2010 to 2020. *Science Robotics*. <https://doi.org/10.1126/scirobotics.abi8017>
- Endiatx. (2025). *Pillbot*. Retrieved May 9, 2025, from <https://endiatx.com/>
- Griffiths, D. J. (2013a). *Introduction to electrodynamics* (4th) [Equation 5.89]. Pearson.
- Griffiths, D. J. (2013b). *Introduction to electrodynamics* (4th) [Equation]. Pearson.
- Griffiths, D. J. (2013c). *Introduction to electrodynamics* (4th) [Equation 6.3]. Pearson.
- Happel, J., & Brenner, H. (1983). *Low reynolds number hydrodynamics* [Equation 2.42]. Martinus Nijhoff Publishers.
- King, R. P. (2002). *Introduction to practical fluid flow*. Butterworth-Heinemann.
- Lamkin-Kennard, K. A., & Popovic, M. B. (2018). Molecular and cellular level—applications in biotechnology and medicine. In *Robotics and automation in the life sciences* (pp. 155–174). Academic Press. <https://doi.org/10.1016/B978-0-12-812939-5.00008-2>
- Salehizadeh, M. (2020). *Control of multiple magnetic microrobots for biomedical applications* [Doctoral dissertation, University of Toronto] [Doctoral dissertation]. <http://hdl.handle.net/1807/103685>
- Shao, Y., Fahmy, A., Li, M., Li, C., Zhao, W., & Sienz, J. (2021). Study on magnetic control systems of micro-robots. *Frontiers in Neuroscience*, 15, 736730. <https://doi.org/10.3389/fnins.2021.736730>

A Source code

Variable names remain in Spanish to preserve consistency with the original research workflow, which was initially conducted in Spanish and later translated into English.

A.1 MATLAB implementation of the P controller (single target)

```
1 function fuera_rango_mayor_P() %P
2     % Basic parameters
3     R = 250e-6;           % Microrobot radius [m]
4     m = 6.545e-7;         % Magnetic moment [A*m^2]
5     mu_m = 0.5;           % Medium viscosity [Pa*s]
6
7     % Calculated constants
8     Omega_t = 2.7271e-17 / mu_m; % [HA^2m^2]
9
10    error_r = 0;
11    error_anterior = 0;
12    psi_i = 0;
13
14    % Control parameters
15    r_deseado = 500e-6;     % Desired radius [m]
16    r_min = 300e-6;        % Lower limit [m]
17    r_max = 700e-6;        % Upper limit [m]
18    K = 0.35;              % Controller gain
19    psi_s = 54.74;         % Equilibrium angle [degrees]
20
21    % Initial conditions
22    r0 = 800e-6;           % Initial radius [m] (out of range)
23    tspan = [0 1];         % Simulation time [s]
24
25    % Solve the dynamics
26    [t, r] = ode45(@(t,r) dynamics(t, r, Omega_t, r_deseado, r_min, r_max,
27    K, psi_i, error_anterior, error_r), tspan, r0);
28
29    % Compute psi at each step
30    psi = zeros(size(r));
31    tipo = zeros(size(r)); % Store control type
32    for i = 1:length(r)
33        [psi(i), tipo(i)] = calculate_psi(r(i), r_deseado, r_min, r_max, K
34        , psi_i, error_anterior, error_r);
35    end
36
37    % Plots
38    figure;
39
40    % 1. Radius plot
41    subplot(2,1,1);
42    hold on;
43    plot(t, r*1e6, 'k', 'LineWidth', 2); % Black solid line
```

```

42 plot(t, r_deseado*1e6*ones(size(t)), 'k--');
43 plot(t, r_min*1e6*ones(size(t)), 'k:');
44 plot(t, r_max*1e6*ones(size(t)), 'k:');
45 xlabel('Time [s]');
46 ylabel('Radius [mu*m]');
47 title('Radius evolution');
48 legend('Current radius', 'Desired radius', 'Control limits', 'Location
    ', 'best');
49 grid on;
50 hold off;
51
52 % 2. Psi angle plot
53 subplot(2,1,2);
54 hold on;
55
56 % Light red semi-transparent background where psi < 0 or psi > 90
57 y_min = -5;
58 y_max = 95;
59 mask = (psi < 0) | (psi > 90);
60 in_zone = false;
61 start_idx = 0;
62
63 for i = 1:length(mask)
64     if mask(i) && ~in_zone
65         start_idx = i;
66         in_zone = true;
67     elseif ~mask(i) && in_zone
68         end_idx = i - 1;
69         fill([t(start_idx:end_idx); flipud(t(start_idx:end_idx))], ...
70             [y_min*ones(end_idx-start_idx+1,1); y_max*ones(end_idx-
71                 start_idx+1,1)], ...
72             [1, 0.8, 0.8], 'EdgeColor', 'none', 'FaceAlpha', 0.5);
73         in_zone = false;
74     end
75 end
76 if in_zone
77     end_idx = length(t);
78     fill([t(start_idx:end_idx); flipud(t(start_idx:end_idx))], ...
79         [y_min*ones(end_idx-start_idx+1,1); y_max*ones(end_idx-
80             start_idx+1,1)], ...
81         [1, 0.8, 0.8], 'EdgeColor', 'none', 'FaceAlpha', 0.5);
82 end
83
84 % Line plotting
85 for i = 1:3
86     idx = tipo == i;
87     switch i
88         case 1
89             plot(t(idx), psi(idx), 'Color', [1, 0.5, 0], 'LineWidth',
90                 2); % orange
91         case 2

```

```

89         plot(t(idx), psi(idx), 'b', 'LineWidth', 2); % blue
90     case 3
91         plot(t(idx), psi(idx), 'g', 'LineWidth', 2); % green
92     end
93 end
94 plot(t, 0*ones(size(t)), 'k--');
95 plot(t, 90*ones(size(t)), 'k--');
96 plot(t, psi_s*ones(size(t)), 'm--');
97 xlabel('Time [s]');
98 ylabel('Control angle psi [degrees]');
99 title('Control Angle psi');
100 ylim([y_min y_max]);
101 grid on;
102 hold off;
103 end
104
105 function drdt = dynamics(t, r, Omega_t, r_deseado, r_min, r_max, K, psi_i,
    error_anterior, error_r)
106 [psi, ~] = calculate_psi(r, r_deseado, r_min, r_max, K, psi_i,
    error_anterior, error_r);
107 psi_rad = deg2rad(psi);
108 drdt = (Omega_t/r^4) * (1 - 3*(cos(psi_rad))^2);
109 end
110
111 function [psi, type] = calculate_psi(r, r_deseado, r_min, r_max, K, psi_i,
    error_anterior, error_r)
112 kp = 0.2;
113 ki = 0;
114 kd = 0;
115 if r < r_min
116     psi = 90;
117     type = 1;
118 elseif r > r_max
119     psi = 0;
120     type = 2;
121 else
122     error_anterior = error_r;
123     error_r = (r - r_deseado)*1e6;
124     psi_p = kp * error_r;
125     psi_i = psi_i + ki * error_r;
126     psi_d = kd * (error_r - error_anterior);
127
128     psi = 54.74 - (psi_p + psi_d + psi_i);
129     type = 3;
130     psi = min(max(0,psi),90);
131 end
132 end

```

Listing 1: MATLAB implementation of the PID controller (single target)

A.2 MATLAB implementation of the PID controller (single target)

```

1 function fuera_rango_mayor_PID() %PID
2     % Basic parameters
3     R = 250e-6;           % Microrobot radius [m]
4     m = 6.545e-7;         % Magnetic moment [A*m^2]
5     mu_m = 0.5;           % Medium viscosity [Pa*s]
6
7     % Calculated constants
8     Omega_t = 2.7271e-17 / mu_m; % [HA^2m^2]
9
10    error_r = 0;
11    error_anterior = 0;
12    psi_i = 0;
13
14    % Control parameters
15    r_deseado = 500e-6;     % Desired radius [m]
16    r_min = 300e-6;        % Lower limit [m]
17    r_max = 650e-6;        % Upper limit [m]
18    K = 0.35;              % Controller gain
19    psi_s = 54.74;         % Equilibrium angle [degrees]
20
21    % Initial conditions
22    r0 = 800e-6;           % Initial radius [m] (out of range)
23    tspan = [0 1];         % Simulation time [s]
24
25    % Solve dynamics
26    [t, r] = ode45(@(t,r) dynamics(t, r, Omega_t, r_deseado, r_min, r_max,
27                                K, psi_i, error_anterior, error_r), tspan, r0);
28
29    % Compute psi at each step
30    psi = zeros(size(r));
31    tipo = zeros(size(r)); % Store control type
32    for i = 1:length(r)
33        [psi(i), tipo(i)] = calculate_psi(r(i), r_deseado, r_min, r_max, K
34                                          , psi_i, error_anterior, error_r);
35    end
36
37    % Plots
38    figure;
39
40    % 1. Radius plot
41    subplot(2,1,1);
42    hold on;
43    plot(t, r*1e6, 'k', 'LineWidth', 2); % Solid black line
44    plot(t, r_deseado*1e6*ones(size(t)), 'k--');
45    plot(t, r_min*1e6*ones(size(t)), 'k:');
46    plot(t, r_max*1e6*ones(size(t)), 'k:');
47    xlabel('Time [s]');
48    ylabel('Radius [mu*m]');

```

```

47 title('Radius Evolution');
48 legend('Current radius', 'Desired radius', 'Control limits', 'Location
    ', 'best');
49 grid on;
50 hold off;
51
52 % 2. Psi angle plot
53 subplot(2,1,2);
54 hold on;
55
56 % Light red semi-transparent background where psi < 0 or psi > 90
57 y_min = -5;
58 y_max = 95;
59 mask = (psi < 0) | (psi > 90);
60 in_zone = false;
61 start_idx = 0;
62
63 for i = 1:length(mask)
64     if mask(i) && ~in_zone
65         start_idx = i;
66         in_zone = true;
67     elseif ~mask(i) && in_zone
68         end_idx = i - 1;
69         fill([t(start_idx:end_idx); flipud(t(start_idx:end_idx))], ...
70             [y_min*ones(end_idx-start_idx+1,1); y_max*ones(end_idx-
71                 start_idx+1,1)], ...
72             [1, 0.8, 0.8], 'EdgeColor', 'none', 'FaceAlpha', 0.5);
73         in_zone = false;
74     end
75 end
76 if in_zone
77     end_idx = length(t);
78     fill([t(start_idx:end_idx); flipud(t(start_idx:end_idx))], ...
79         [y_min*ones(end_idx-start_idx+1,1); y_max*ones(end_idx-
80             start_idx+1,1)], ...
81         [1, 0.8, 0.8], 'EdgeColor', 'none', 'FaceAlpha', 0.5);
82 end
83
84 % Line plotting
85 for i = 1:3
86     idx = tipo == i;
87     switch i
88     case 1
89         plot(t(idx), psi(idx), 'Color', [1, 0.5, 0], 'LineWidth',
90             2); % orange
91     case 2
92         plot(t(idx), psi(idx), 'b', 'LineWidth', 2); % blue
93     case 3
94         plot(t(idx), psi(idx), 'g', 'LineWidth', 2); % green
95     end
96 end

```

```

94     plot(t, 0*ones(size(t)), 'k--');
95     plot(t, 90*ones(size(t)), 'k--');
96     plot(t, psi_s*ones(size(t)), 'm--');
97     xlabel('Time [s]');
98     ylabel('Control angle psi [degrees]');
99     title('Control Angle psi');
100    ylim([y_min y_max]);
101    grid on;
102    hold off;
103 end
104
105 function drdt = dynamics(t, r, Omega_t, r_deseado, r_min, r_max, K, psi_i,
    error_anterior, error_r)
106     [psi, ~] = calculate_psi(r, r_deseado, r_min, r_max, K, psi_i,
        error_anterior, error_r);
107     psi_rad = deg2rad(psi);
108     drdt = (Omega_t/r^4) * (1 - 3*(cos(psi_rad))^2);
109 end
110
111 function [psi, type] = calculate_psi(r, r_deseado, r_min, r_max, K, psi_i,
    error_anterior, error_r)
112     kp = 0.2;
113     ki = 0.18;
114     kd = 0.2;
115     if r < r_min
116         psi = 90;
117         type = 1;
118     elseif r > r_max
119         psi = 0;
120         type = 2;
121     else
122         error_anterior = error_r;
123         error_r = (r - r_deseado)*1e6;
124         psi_p = kp * error_r;
125         psi_i = psi_i + ki * error_r;
126         psi_d = kd * (error_r - error_anterior);
127
128         psi = 54.74 - (psi_p + psi_d + psi_i);
129         type = 3;
130         psi = min(max(0,psi),90);
131     end
132 end

```

Listing 2: MATLAB implementation of the PID controller (single target)

A.3 MATLAB implementation of the PID controller with multiple target radii

```

1 function radios_cambiantes_PID() % Multiple-radius PID controller

```

```

2 % Basic parameters
3 R = 250e-6; % Microrobot radius [m]
4 m = 6.545e-7; % Magnetic moment [A*m^2]
5 mu_m = 0.5; % Medium viscosity [Pa*s]
6
7 % Calculated constants
8 Omega_t = 2.7271e-17 / mu_m; % [HA^2*m^2]
9
10 error_r = 0;
11 error_anterior = 0;
12 psi_i = 0;
13
14 % Control parameters
15 r_deseado_inicial = 500e-6; % Initial desired radius [m]
16 r_min = 300e-6; % Lower limit [m]
17 r_max = 700e-6; % Upper limit [m]
18 K = 0.35; % Controller gain
19 psi_s = 54.74; % Equilibrium angle [degrees]
20
21 % Initial conditions
22 r0 = 800e-6; % Initial radius [m] (outside range)
23 tspan = [0 5]; % Simulation time [s] (extended to
    observe multiple changes)
24
25 % Define desired radius changes every second
26 r_deseado_valores = [500e-6, 400e-6, 600e-6, 550e-6, 450e-6]; %
    Desired radius sequence
27
28 % Solve system dynamics with varying desired radius
29 options = odeset('OutputFcn', @odeplot);
30 [t, r] = ode45(@(t,r) dynamics(t, r, Omega_t, get_current_r_deseado(t,
    r_deseado_inicial, r_deseado_valores),...
31 r_min, r_max, K, psi_i, error_anterior,
    error_r), tspan, r0);
32
33 % Compute psi for each step
34 psi = zeros(size(r));
35 tipo = zeros(size(r)); % Store control type
36 r_deseado_actual = zeros(size(r)); % Store current desired radius
37 for i = 1:length(r)
38     current_time = t(i);
39     current_r_deseado = get_current_r_deseado(current_time,
        r_deseado_inicial, r_deseado_valores);
40     r_deseado_actual(i) = current_r_deseado;
41     [psi(i), tipo(i)] = calculate_psi(r(i), current_r_deseado, r_min,
        r_max, K, psi_i, error_anterior, error_r);
42 end
43
44 % ----- Plot results -----
45 figure;
46

```

```

47 % 1. Radius evolution plot
48 subplot(2,1,1);
49 hold on;
50 plot(t, r*1e6, 'k', 'LineWidth', 2); % Solid black
    line
51 plot(t, r_deseado_actual*1e6, 'r--', 'LineWidth', 1.5); % Red dashed
    line for variable desired radius
52 plot(t, r_min*1e6*ones(size(t)), 'k:');
53 plot(t, r_max*1e6*ones(size(t)), 'k:');
54 xlabel('Time [s]');
55 ylabel('Radius [mu*m]');
56 title('Radius Evolution');
57 legend('Current radius', 'Desired radius (variable)', 'Control limits'
    , 'Location', 'best');
58 grid on;
59 hold off;
60
61 % 2. psi (control angle) plot
62 subplot(2,1,2);
63 hold on;
64
65 % Light red shaded background where psi < 0 or psi > 90
66 y_min = -5;
67 y_max = 95;
68 mask = (psi < 0) | (psi > 90);
69 in_zone = false;
70 start_idx = 0;
71
72 for i = 1:length(mask)
73     if mask(i) && ~in_zone
74         start_idx = i;
75         in_zone = true;
76     elseif ~mask(i) && in_zone
77         end_idx = i - 1;
78         fill([t(start_idx:end_idx); flipud(t(start_idx:end_idx))], ...
79             [y_min*ones(end_idx-start_idx+1,1); y_max*ones(end_idx-
            start_idx+1,1)], ...
80             [1, 0.8, 0.8], 'EdgeColor', 'none', 'FaceAlpha', 0.5);
81         in_zone = false;
82     end
83 end
84 if in_zone
85     end_idx = length(t);
86     fill([t(start_idx:end_idx); flipud(t(start_idx:end_idx))], ...
87         [y_min*ones(end_idx-start_idx+1,1); y_max*ones(end_idx-
            start_idx+1,1)], ...
88         [1, 0.8, 0.8], 'EdgeColor', 'none', 'FaceAlpha', 0.5);
89 end
90
91 % Line plotting
92 for i = 1:3

```



```

93     idx = tipo == i;
94     switch i
95     case 1
96         plot(t(idx), psi(idx), 'Color', [1, 0.5, 0], 'LineWidth',
97             2); % orange
98     case 2
99         plot(t(idx), psi(idx), 'b', 'LineWidth', 2); % blue
100    case 3
101        plot(t(idx), psi(idx), 'g', 'LineWidth', 2); % green
102    end
103    plot(t, 0*ones(size(t)), 'k--');
104    plot(t, 90*ones(size(t)), 'k--');
105    plot(t, psi_s*ones(size(t)), 'm--');
106    xlabel('Time [s]');
107    ylabel('Control angle psi [degrees]');
108    title('Control Angle psi');
109    ylim([y_min y_max]);
110    grid on;
111    hold off;
112 end
113
114 function drdt = dynamics(t, r, Omega_t, r_deseado, r_min, r_max, K, psi_i,
115     error_anterior, error_r)
116     [psi, ~] = calculate_psi(r, r_deseado, r_min, r_max, K, psi_i,
117         error_anterior, error_r);
118     psi_rad = deg2rad(psi);
119     drdt = (Omega_t/r^4) * (1 - 3*(cos(psi_rad))^2);
120 end
121
122 function [psi, type] = calculate_psi(r, r_deseado, r_min, r_max, K, psi_i,
123     error_anterior, error_r)
124     kp = 0.2;
125     ki = 0.18;
126     kd = 0.2;
127     if r < r_min
128         psi = 90;
129         type = 1;
130     elseif r > r_max
131         psi = 0;
132         type = 2;
133     else
134         error_anterior = error_r;
135         error_r = (r - r_deseado)*1e6;
136         psi_p = kp * error_r;
137         psi_i = psi_i + ki * error_r;
138         psi_d = kd * (error_r - error_anterior);
139         psi = 54.74 - (psi_p + psi_d + psi_i);
140         type = 3;
141         psi = min(max(0, psi), 90);

```

```

140     end
141 end
142
143 % Auxiliary function to obtain the current desired radius based on time
144 function r_deseado = get_current_r_deseado(t, r_deseado_inicial,
    r_deseado_valores)
145     % Change the desired radius every second
146     segundo_actual = floor(t) + 1; % +1 because MATLAB indexes from 1
147     if segundo_actual > length(r_deseado_valores)
148         segundo_actual = length(r_deseado_valores);
149     end
150     r_deseado = r_deseado_valores(segundo_actual);
151 end

```

Listing 3: MATLAB implementation of the PID controller with multiple target radii

A.4 MATLAB implementation of the cascade PID+PD controller with multiple target radii

```

1 function radios_cambiantes_PIDCC() % Multiple-radius Cascade PID
    controller
2     % Basic parameters
3     R = 250e-6;           % Microrobot radius [m]
4     m = 6.545e-7;         % Magnetic moment [A*m^2]
5     mu_m = 0.5;           % Medium viscosity [Pa*s]
6
7     % Calculated constants
8     Omega_t = 2.7271e-17 / mu_m; % [HA^2*m^2]
9
10    error_r = 0;
11    error_anterior = 0;
12    psi_i = 0;
13
14    % Control parameters
15    r_deseado_inicial = 500e-6; % Initial desired radius [m]
16    r_min = 300e-6;           % Lower limit [m]
17    r_max = 700e-6;           % Upper limit [m]
18    K = 0.35;                 % Controller gain
19    psi_s = 54.74;            % Equilibrium angle [degrees]
20
21    % Initial conditions
22    r0 = 800e-6;              % Initial radius [m] (outside range)
23    tspan = [0 5];           % Extended simulation time to observe
        transitions
24
25    % Define desired radius changes every second
26    r_deseado_valores = [500e-6, 400e-6, 600e-6, 550e-6, 450e-6]; %
        Desired radius sequence
27

```

```

28 % Solve dynamics with changing desired radius
29 options = odeset('OutputFcn', @odeplot);
30 [t, r] = ode45(@(t,r) dynamics(t, r, Omega_t, get_current_r_deseado(t,
31     r_deseado_inicial, r_deseado_valores),...
32     r_min, r_max, K, psi_i, error_anterior,
33     error_r), tspan, r0);
34
35 % Compute psi for each time step
36 psi = zeros(size(r));
37 tipo = zeros(size(r)); % Store control type
38 r_deseado_actual = zeros(size(r)); % Store current desired radius
39 for i = 1:length(r)
40     current_time = t(i);
41     current_r_deseado = get_current_r_deseado(current_time,
42         r_deseado_inicial, r_deseado_valores);
43     r_deseado_actual(i) = current_r_deseado;
44     [psi(i), tipo(i)] = calculate_psi(r(i), current_r_deseado, r_min,
45         r_max, K, psi_i, error_anterior, error_r);
46 end
47
48 % ----- Plot results -----
49 figure;
50
51 % 1. Radius evolution plot
52 subplot(2,1,1);
53 hold on;
54 plot(t, r*1e6, 'k', 'LineWidth', 2); % Solid black
55 line
56 plot(t, r_deseado_actual*1e6, 'r--', 'LineWidth', 1.5); % Red dashed
57 line for variable desired radius
58 plot(t, r_min*1e6*ones(size(t)), 'k:');
59 plot(t, r_max*1e6*ones(size(t)), 'k:');
60 xlabel('Time [s]');
61 ylabel('Radius [mu*m]');
62 title('Radius Evolution');
63 legend('Current radius', 'Desired radius (variable)', 'Control limits',
64     , 'Location', 'best');
65 grid on;
66 hold off;
67
68 % 2. Control angle psi plot
69 subplot(2,1,2);
70 hold on;
71
72 % Light red shaded background where psi < 0 or psi > 90
73 y_min = -5;
74 y_max = 95;
75 mask = (psi < 0) | (psi > 90);
76 in_zone = false;
77 start_idx = 0;

```

```

72     for i = 1:length(mask)
73         if mask(i) && ~in_zone
74             start_idx = i;
75             in_zone = true;
76         elseif ~mask(i) && in_zone
77             end_idx = i - 1;
78             fill([t(start_idx:end_idx); flipud(t(start_idx:end_idx))], ...
79                 [y_min*ones(end_idx-start_idx+1,1); y_max*ones(end_idx-
80                     start_idx+1,1)], ...
81                 [1, 0.8, 0.8], 'EdgeColor', 'none', 'FaceAlpha', 0.5);
82             in_zone = false;
83         end
84     end
85     if in_zone
86         end_idx = length(t);
87         fill([t(start_idx:end_idx); flipud(t(start_idx:end_idx))], ...
88             [y_min*ones(end_idx-start_idx+1,1); y_max*ones(end_idx-
89                 start_idx+1,1)], ...
90             [1, 0.8, 0.8], 'EdgeColor', 'none', 'FaceAlpha', 0.5);
91     end
92     % Line plotting by control type
93     for i = 1:3
94         idx = tipo == i;
95         switch i
96             case 1
97                 plot(t(idx), psi(idx), 'Color', [1, 0.5, 0], 'LineWidth',
98                     2); % orange
99             case 2
100                 plot(t(idx), psi(idx), 'b', 'LineWidth', 2); % blue
101             case 3
102                 plot(t(idx), psi(idx), 'g', 'LineWidth', 2); % green
103         end
104     end
105     plot(t, 0*ones(size(t)), 'k--');
106     plot(t, 90*ones(size(t)), 'k--');
107     plot(t, psi_s*ones(size(t)), 'm--');
108     xlabel('Time [s]');
109     ylabel('Control angle psi [degrees]');
110     title('Control Angle psi');
111     ylim([y_min y_max]);
112     grid on;
113     hold off;
114 end
115
116 function drdt = dynamics(t, r, Omega_t, r_deseado, r_min, r_max, K, psi_i,
117     error_anterior, error_r)
118     [psi, ~] = calculate_psi(r, r_deseado, r_min, r_max, K, psi_i,
119         error_anterior, error_r);
120     psi_rad = deg2rad(psi);
121     drdt = (Omega_t/r^4) * (1 - 3*(cos(psi_rad))^2);

```

```

118 end
119
120 function [psi, type] = calculate_psi(r, r_deseado, r_min, r_max, K, psi_i,
    error_anterior, error_r)
121 persistent psi_aplicado psi_i_c e_anterior psi_anterior e
122 if isempty(psi_aplicado)
123     psi_aplicado = 54.74;
124     psi_i_c = 0;
125     e_anterior = 0;
126     psi_anterior = 54.74;
127     e = 0;
128 end
129
130 % --- PID to compute target psi ---
131 kp = 0.2;
132 ki = 0.18;
133 kd = 0.2;
134
135 if r < r_min
136     psi_objetivo = 90;
137     type = 1;
138 elseif r > r_max
139     psi_objetivo = 0;
140     type = 2;
141 else
142     error_anterior = error_r;
143     error_r = (r - r_deseado)*1e6;
144     psi_p = kp * error_r;
145     psi_i = psi_i + ki * error_r;
146     psi_d = kd * (error_r - error_anterior);
147
148     psi_objetivo = 54.74 - (psi_p + psi_d + psi_i);
149     type = 3;
150 end
151 psi_objetivo = min(max(0, psi_objetivo), 90);
152
153 % --- Cascade PID to smooth psi response ---
154 kpc = 0.7;
155 kic = 0;
156 kdc = 0.05;
157
158 e_anterior = e;
159 e = psi_aplicado - psi_objetivo;
160 psi_p_c = kpc * e;
161 psi_i_c = psi_i_c + kic * e;
162 psi_d_c = kdc * (e - e_anterior);
163
164 psi_aplicado = psi_aplicado - (psi_p_c + psi_d_c + psi_i_c);
165 psi_aplicado = min(max(0, psi_aplicado), 90);
166
167 % Update internal state

```

```

168     e_anterior = e;
169     psi_anterior = psi_aplicado;
170
171     psi = psi_aplicado;
172 end
173
174 % Auxiliary function to obtain the current desired radius based on time
175 function r_deseado = get_current_r_deseado(t, r_deseado_inicial,
    r_deseado_valores)
176     % Change the desired radius every second
177     segundo_actual = floor(t) + 1; % +1 because MATLAB indexes from 1
178     if segundo_actual > length(r_deseado_valores)
179         segundo_actual = length(r_deseado_valores);
180     end
181     r_deseado = r_deseado_valores(segundo_actual);
182 end

```

Listing 4: MATLAB implementation of the cascade PID+PD controller with multiple target radii